

## LHC luminosity and energy upgrades confront natural supersymmetry models

Howard Baer,<sup>1,\*</sup> Vernon Barger,<sup>2,†</sup> James S. Gainer,<sup>3,‡</sup> Dibyashree Sengupta,<sup>1,§</sup> Hasan Serce,<sup>1,||</sup> and Xerxes Tata<sup>3,4,¶</sup>

<sup>1</sup>*Department of Physics and Astronomy, University of Oklahoma, Norman, Oklahoma 73019, USA*

<sup>2</sup>*Department of Physics, University of Wisconsin, Madison, Wisconsin 53706, USA*

<sup>3</sup>*Department of Physics and Astronomy, University of Hawaii, Honolulu, Hawaii 96822, USA*

<sup>4</sup>*Centre for High Energy Physics, Indian Institute of Science, Bangalore 560012, India*



(Received 21 August 2018; published 12 October 2018)

The electroweak fine-tuning measure  $\Delta_{EW}$  allows for correlated supersymmetry (SUSY) soft terms as are expected in any ultraviolet complete theory. Requiring no less than 3% electroweak fine-tuning implies upper bounds of about 360 GeV on all Higgsinos, while top squarks are lighter than  $\sim 3$  TeV and gluinos are bounded by  $\sim 6$ – $9$  TeV. We examine the reach for SUSY of the planned high luminosity (HL:  $3 \text{ ab}^{-1}$  at 14 TeV) and the proposed high energy (HE:  $15 \text{ ab}^{-1}$  at 27 TeV) upgrades of the LHC via four LHC collider search channels relevant for natural SUSY: 1. gluino pair production followed by gluino decay to third generation (s)quarks, 2. top squark pair production followed by decay to third generation quarks and light Higgsinos, 3. neutral Higgsino pair production with QCD jet radiation (resulting in monojet events with soft dileptons), and 4. wino pair production followed by decay to light Higgsinos leading to same-sign diboson production. We confront our reach results with upper limits on superpartner masses in four natural SUSY models: natural gravity mediation via the 1. two- and 2. three-extra-parameter nonuniversal Higgs models, 3. natural minilandscape models with generalized mirage mediation and 4. natural anomaly mediation. We find that while the HL-LHC can probe considerable portions of natural SUSY parameter space in all these models, the HE-LHC will decisively cover the entire natural SUSY parameter space with better than 3% fine-tuning.

DOI: [10.1103/PhysRevD.98.075010](https://doi.org/10.1103/PhysRevD.98.075010)

### I. INTRODUCTION

With the discovery of the Higgs boson in 2012 [1], the CERN LHC has verified the particle content of the standard model (SM). In spite of this impressive triumph, many physicists still expect new physics to be revealed at the LHC. The primary reason is the instability of the SM Higgs boson mass under radiative corrections if the SM is embedded into a high scale theory (such as string theory). Starting with the SM scalar potential

$$V = -\mu^2 \phi^\dagger \phi + \lambda (\phi^\dagger \phi)^2, \quad (1)$$

one finds the Higgs mass, including leading radiative corrections cutoff at an energy scale  $\Lambda$  (where new physics degrees of freedom not present in the SM become important), to be

$$m_h^2 \simeq 2\mu^2 + \delta m_h^2,$$

with<sup>1</sup>

$$\delta m_h^2 \simeq \frac{3}{4\pi^2} \left( -\lambda_t^2 + \frac{g^2}{4} + \frac{g^2}{8\cos^2\theta_W} + \lambda \right) \Lambda^2. \quad (2)$$

Here,  $\lambda_t$  is the top quark Yukawa coupling given in the SM by  $\lambda_t = \frac{gm_t}{\sqrt{2}M_W}$ ,  $g$  is the  $SU(2)_L$  gauge coupling,  $\theta_W$  is the Weinberg angle and  $\lambda$  is the Higgs quartic coupling in the Higgs boson potential (1). The quadratic sensitivity of the SM Higgs boson mass to new physics at the high

<sup>1</sup>Quadratic divergences in the SM were studied by Veltman [2]. While the use of a cutoff as a regulator is not gauge invariant, the coefficient of  $\Lambda^2$  in Eq. (2) is independent of  $\xi$  in  $R_\xi$  gauges. For subtleties on the regulation scheme dependence of the quadratic sensitivity of the Higgs boson mass to high scale physics, see Ref. [3].

\*baer@nhn.ou.edu

†barger@pheno.wisc.edu

‡jgainer@hawaii.edu

§Dibyashree.Sengupta-1@ou.edu

||serce@ou.edu

¶tata@phys.hawaii.edu

*Published by the American Physical Society under the terms of the Creative Commons Attribution 4.0 International license. Further distribution of this work must maintain attribution to the author(s) and the published article's title, journal citation, and DOI. Funded by SCOAP<sup>3</sup>.*

scale  $\Lambda$  embodies the fine-tuning problem of the SM. If the new physics scale  $\Lambda \gg 1$  TeV, then the *free* parameter  $\mu^2$  will have to be accordingly fine-tuned to maintain the Higgs mass at its measured value  $m_h = 125.09 \pm 0.24$  GeV [4]. The fine-tuning gets consequently more implausible as the theory cutoff  $\Lambda$  extends significantly beyond the weak scale. The need for large fine-tuning suggests a missing ingredient in the underlying theory because otherwise seemingly *independent* contributions to the Higgs boson mass would then need to have large unexplained cancellations in order to yield its measured value.

Perhaps the most elegant and compelling resolution [5] of the fine-tuning problem is to extend the underlying Poincaré spacetime symmetries to the more general super-Poincaré group. In the supersymmetrized version of the SM, along with weak scale soft supersymmetry (SUSY) breaking terms [the so-called minimal supersymmetric standard model (MSSM) [6]], the quadratic cutoff dependence seen in Eq. (2) is absent, leaving only relatively mild but intertwined logarithmic sensitivity to high scale physics. In addition to including a cure for the divergent Higgs mass, the MSSM receives impressive support from *data* via several different virtual effects.

- (i) The measured values of gauge coupling constants are consistent with unification under renormalization group running within the MSSM [7,8],
- (ii) the measured value of the top quark mass is within the range required to trigger a radiatively driven breakdown of electroweak symmetry [9], and
- (iii) the measured value of the Higgs mass fall squarely with the narrow window of MSSM prediction [10], and in fact agrees with the radiatively corrected MSSM  $m_h$  calculation provided top squarks ( $\tilde{t}_{1,2}$ ) lie in the TeV range and are highly mixed by TeV-scale trilinear soft terms [11].

The *natural* MSSM seemingly requires the existence of several superpartners (those that have direct couplings to the Higgs sector) with masses not too far beyond the weak scale as typified by  $m_{\text{weak}} \simeq m_{W,Z,h} \sim 100$  GeV [6]. So far, searches by LHC experiments have failed to find any superpartners leading to simplified model gluino ( $\tilde{g}$ ) mass limits such as  $m_{\tilde{g}} \gtrsim 2$  TeV [12,13] and top squark ( $\tilde{t}_1$ ) mass limits such as  $m_{\tilde{t}_1} \gtrsim 1.1$  TeV [14,15]—along with considerably weaker limits on electroweakly interacting superpartners. The widening mass gap between the weak scale and the soft breaking scale has seemingly sharpened the issue of a *little hierarchy*: how can it be that  $m_{\text{weak}} \ll m_{\text{soft}}$  when the soft breaking scale is supposed to determine the weak scale? Naively, one might expect  $m_{\text{weak}} \sim m_{\text{soft}}$  absent again any fine-tuning. Indeed, early estimates of naturalness or lack of fine-tuning within SUSY models seemed to require  $m_{\tilde{g}} \lesssim 350$  GeV and  $m_{\tilde{t}_1} \lesssim 400$  GeV for no worse than 3% fine-tuning [16–18]. Some more recent naturalness calculations seemed to require *three* third generation

squarks with mass below about 500 GeV [19]. The contrast between these naturalness bounds and current LHC mass limits might indicate a need to fine-tune within the MSSM to maintain  $m_{\text{weak}} \sim 100$  GeV which in turn may signal some pathology or missing ingredient this time within the SUSY paradigm.

An issue with these estimates is that they ignore the possibility that model parameters—usually taken to be independent in order to parametrize our ignorance of SUSY breaking—should be correlated (interdependent) in ultraviolet complete theories. Such correlations can lead to automatic cancellations between terms involving large logarithms: thus, ignoring this possibility can easily lead to large overestimates of the UV sensitivity of the theory [20–22].

To allow for the fact that the underlying model parameters are expected to be correlated, we adopt the very conservative fine-tuning measure,  $\Delta_{\text{EW}}$  [23,24]. The quantity  $\Delta_{\text{EW}}$  measures how well the *weak scale* MSSM Lagrangian parameters match the measured value of the weak scale. By minimizing the MSSM weak scale scalar potential to determine the Higgs field vacuum expectation values (VEVs), one derives the well-known expression relating the  $Z$ -boson mass to the SUSY Lagrangian parameters,

$$\frac{m_Z^2}{2} = \frac{m_{H_d}^2 + \Sigma_d^d - (m_{H_u}^2 + \Sigma_u^u) \tan^2 \beta}{\tan^2 \beta - 1} - \mu^2 \simeq -m_{H_u}^2 - \Sigma_u^u(\tilde{t}_{1,2}) - \mu^2. \quad (3)$$

Here,  $\tan \beta = v_u/v_d$  is the ratio of Higgs field vacuum expectation values and the  $\Sigma_u^u$  and  $\Sigma_d^d$  contain an assortment of radiative corrections, the largest of which typically arise from the top squarks. Expressions for the  $\Sigma_u^u$  and  $\Sigma_d^d$  are given in the Appendix of Ref. [24]. Thus,  $\Delta_{\text{EW}}$  compares the maximal contribution on the right-hand side (rhs) of Eq. (3) to the value of  $m_Z^2/2$ . If the magnitudes of the terms on the rhs of Eq. (3) are individually comparable to  $m_Z^2/2$ , then no unnatural fine-tunings are required to generate  $m_Z = 91.2$  GeV. We have shown that once appropriate interparameter correlations are properly taken into account [20–22], the traditional fine-tuning measure [16],  $\Delta_{\text{BG}} \equiv \max_i \left| \frac{\partial \log m_Z^2}{\partial \log p_i} \right|$ , indeed reduces to  $\Delta_{\text{EW}}$ .

A utilitarian feature of the naturalness calculation is that it leads to upper bounds on sparticle masses which in turn provide targets for present or future colliding beam experiments that seek to discover superpartners or falsify the weak scale SUSY hypothesis. But for which values of  $\Delta_{\text{EW}}$  is SUSY natural? The original calculations of Barbieri-Giudice used  $\Delta_{\text{BG}} < 10$ , or no less than  $\Delta_{\text{BG}}^{-1} = 10\%$  fine-tuning. We, more conservatively, adopt a value  $\Delta_{\text{EW}} < 30$  (3.3% electroweak fine-tuning) as an upper bound on natural SUSY models.<sup>2</sup> That this is a qualitatively different

<sup>2</sup>The onset of fine-tuning for  $\Delta_{\text{EW}} > 20$ –30 is visually displayed in Ref. [25].

criterion is driven home by the fact that it is possible to have the same model with both  $\Delta_{EW} < 30$  and  $\Delta_{BG} > 3000$  (if the latter is naively evaluated with multiple uncorrelated soft terms [21]).

Natural models with low electroweak fine-tuning ( $\Delta_{EW} \lesssim 30$ ) exhibit the following features:

- (i)  $|\mu| \sim 100\text{--}350$  GeV [26,27] (the lighter the better) where  $\mu \gtrsim 100$  GeV is required to accommodate LEP2 limits from chargino pair production searches.<sup>3</sup>
- (ii)  $m_{H_u}^2$  is driven radiatively to small—not large—negative values at the weak scale (radiatively driven naturalness) [23,24].
- (iii) The top squark contributions to the radiative corrections  $\Sigma_u^u(\tilde{t}_{1,2})$  are minimized for TeV-scale highly mixed top squarks [23]. This latter condition also lifts the Higgs mass to  $m_h \sim 125$  GeV. For  $\Delta_{EW} \lesssim 30$ , the lighter top squarks are bounded by  $m_{\tilde{t}_1} \lesssim 3$  TeV [24,25].
- (iv) The gluino mass, which feeds into the top squark masses at one loop and hence into the scalar potential at two-loop order, is bounded by  $m_{\tilde{g}} \lesssim 6\text{--}9$  TeV [24,25] (depending on the details of the model).

These new sparticle mass bounds derived from the  $\Delta_{EW}$  measure lie well beyond current LHC search limits and allow for the possibility that SUSY is still natural and still awaiting discovery. The question then is: how far along are LHC SUSY searches on their way to discovering or falsifying supersymmetry? And what sort of LHC upgrade is needed to either discover or falsify natural SUSY? Indeed, recently the European Strategy Study has begun to assess what sort of accelerator (or other experiments) are needed beyond high-luminosity LHC (HL-LHC). One option is to double the field strength of the dipole steering magnets to 16 Tesla. This would allow for an energy upgrade of LHC to  $\sqrt{s} = 27$  TeV with an assumed  $15 \text{ ab}^{-1}$  of integrated luminosity (HE-LHC). The goal of this paper is to reexamine the SUSY theory/experiment confrontation with a view to informing these questions about future experiments and to examine what collider options are needed to completely probe the natural SUSY parameter space. In doing so, we confront four different natural SUSY models with updated LHC limits from four SUSY search channels that are deemed most important for discovering/falsifying natural supersymmetry.

The four natural SUSY models we examine here include the following:

- (i) Natural gravity mediation as exhibited in the two- and three-extra-parameter nonuniversal Higgs model (nNUHM2 and nNUHM3) [28]. The NUHM2 model has parameter space  $m_0, m_{1/2}, A_0, \tan \beta, \mu, m_A$ , which allows for the required light Higgsinos since the superpotential  $\mu$  parameter is now a freely adjustable

<sup>3</sup>We assume that the superpotential  $\mu$ -term makes the dominant contribution to the Higgsino mass.

input parameter so that the necessary naturalness requirement that  $\mu \lesssim 350$  GeV is easily obtained. The nNUHM2,3 models assume gaugino mass unification, which under MSSM renormalization group evolution leads to weak scale gauginos in the mass ratio  $M_1 : M_2 : M_3 \sim 1 : 2 : 7$  while naturalness requires  $\mu < M_1 < M_2 < M_3$  so that a Higgsino-like WIMP is the lightest SUSY particle (LSP). The nNUHM3 model has the added feature that first/second generation matter scalars need not be degenerate with third generation scalars. This sort of feature emerges in top-down SUSY models such as the natural minilandscape [29,30].

- (ii) Natural (generalized) anomaly mediation or nAMSB adopts the usual anomaly-mediated supersymmetry breaking (AMSB) masses but also allows for *non-universal* bulk Higgs masses  $m_{H_u}$  and  $m_{H_d}$  as compared to bulk matter scalar masses  $m_0$  [31]. It also includes some bulk trilinear  $A_0$  soft term contributions. The parameter space is then  $m_0, m_{3/2}, A_0, \tan \beta, \mu, m_A$ . The nonuniversal and trilinear bulk terms allow for  $m_h \simeq 125$  GeV while allowing for naturalness in the spectra. For nAMSB, the electroweakinos are oriented such that  $\mu < M_2 < M_1 < M_3$  at the weak scale. The LSP in nAMSB is a Higgsino-like LSP instead of winolike as is typically assumed. For greater generality, one may include as well separate first/second versus third generation bulk matter scalar masses  $m_0(1, 2)$  and  $m_0(3)$ .
- (iii) Natural generalized mirage mediation (nGMM) models [32], in which one expects comparable anomaly- and modulus/gravity-mediated contributions to soft breaking terms. The nGMM parameter space [33] is  $\alpha, m_{3/2}, c_m, c_{m3}, a_3, \tan \beta, \mu, m_A$ , where  $\alpha$  parametrizes the relative modulus-to-anomaly-mediation contributions and the  $c_m, c_{m3}$  and  $a_3$  are continuous generalizations of previous discrete parameters related to modular weights. Since gaugino masses unify at some intermediate (mirage) scale  $\mu_{mir} = e^{-8\pi^2/\alpha} m_{GUT}$ , the gaugino masses are *compressed* compared to NUHM2 (3) so one expects  $\mu \ll M_1 \lesssim M_2 \lesssim M_3$ . As an example, we examine the minilandscape picture taking  $m_{3/2} \simeq m_0(1, 2) > 2 \times m_0(3)$  [30].

These four models have been encoded in Isajet v7.88 [34] which we use for spectra generation and the  $\Delta_{EW}$  calculation. For each of the four models, we scan over the whole parameter space (with  $\tan \beta$ : 3–60) and accept solutions that are consistent with current LHC sparticle mass constraints, with  $m_h = 125 \pm 2$  GeV (adopting  $\sim \pm 2$  GeV theory error in our Higgs mass calculation). The parameter scan limits for each model are shown in Table I. We also require that solutions have  $\Delta_{EW} < 30$  in order to satisfy naturalness—which amounts to a reasonable SUSY model prediction for the magnitude of the weak scale. For the nGMM parameter space, we require  $\alpha$  to be positive (real

TABLE I. Scan limits for various parameters in the natural SUSY models considered here. Parameter definitions can be found in the references for nNUHM2,3 [28], nAMSB [31] and nGMM [30,33]. For each model, we also allow  $\tan\beta$ : 3–60,  $\mu$ : 100–360 GeV and  $m_A$ : 0.3–10 TeV.

nNUHM2	nNUHM3	nAMSB	nGMM (minilandscape)
$m_0$ : 0.1–15 TeV	$m_0(1, 2)$ : 0.1–40 TeV	$m_0(1, 2)$ : 0.1–40 TeV	$\alpha$ : 0–40
	$m_0(3)$ : 0.1–15 TeV	$m_0(3)$ : 0.1–15 TeV	$c_{m3} < c_m/4$
$m_{1/2}$ : 0.5–3 TeV	$m_{1/2}$ : 0.5–3 TeV	$m_{3/2}$ : 60–500 TeV	$m_{3/2}$ : 1–35 TeV
$A_0$ : $-30 \rightarrow +30$ TeV	$A_0$ : $-30 \rightarrow +30$ TeV	$A_0$ : $-35 \rightarrow +15$ TeV	$a_3$ : $-20 \rightarrow +20$
			$c_m = (16\pi^2/\alpha)^2$

mirage unification) and  $\alpha < 40$  so that anomaly mediation is not highly suppressed.

The four most important search channels for natural SUSY at the LHC or its upgrades are the following.<sup>4</sup>

- (i) Gluino pair production  $pp \rightarrow \tilde{g}\tilde{g}X$  followed by either two-body gluino decay to top squarks  $\tilde{g} \rightarrow \tilde{t}^*t$ ,  $\tilde{t}_1\tilde{t}$  or, if these are closed, then gluino three-body decays to mainly third generation quarks [39]:  $\tilde{g} \rightarrow t\tilde{t}\tilde{Z}_i$ ,  $b\tilde{b}\tilde{Z}_i$  or  $t\tilde{b}\tilde{W}_j^+ + c.c.$
- (ii) Top squark pair production  $pp \rightarrow \tilde{t}_1\tilde{t}_1^*X$  followed by  $\tilde{t}_1 \rightarrow t\tilde{Z}_i$  or  $b\tilde{W}_j^+$  [40].
- (iii) Higgsino pair production via  $pp \rightarrow \tilde{Z}_i\tilde{Z}_j$ ,  $\tilde{W}_1\tilde{Z}_i$ ,  $\tilde{W}_1\tilde{W}_j$  channels is unlikely to be visible above SM  $Zj$  background because the signal to background ratio is just 1%–2% [41]. However, the  $pp \rightarrow \tilde{Z}_1\tilde{Z}_2j$  channel (with contributions from  $pp \rightarrow \tilde{W}_1\tilde{Z}_2j$ ), where  $\tilde{Z}_2 \rightarrow \ell\bar{\ell}\tilde{Z}_1$  with a soft OS dilepton pair and where the hard initial state radiated jet supplies a trigger, offers a promising search channel for low mass Higgsinos with  $m_{\tilde{Z}_{1,2}} \sim 100$ –300 GeV [42]. Indeed, the LHC collaborations have presented their first results for this search [43,44], and it is especially encouraging that the ATLAS collaboration is able to access a  $\tilde{Z}_2 - \tilde{Z}_1$  mass gap as small as 2.5 GeV.
- (iv) Wino pair production  $pp \rightarrow \tilde{W}_2^\pm\tilde{Z}_{3\text{ or }4}X$  followed by  $\tilde{W}_2 \rightarrow W\tilde{Z}_{1,2}$  and  $\tilde{Z}_{3\text{ or }4} \rightarrow W^\pm\tilde{W}_1^\mp$ . Half the time, this final state leads to a same-sign diboson (SSdB) final state that, when followed by leptonic  $W$  decays, leads to same-sign dileptons +MET with very little accompanying jet activity [45] (as opposed to SS dileptons arising from gluino cascade decays). The SSdB signature has very low SM background rates arising mainly from  $t\bar{t}W$  production.

In Sec. II, we present our updated reach projections for revised HE-LHC specifications with  $\sqrt{s} = 27$  TeV and a

<sup>4</sup>Precision measurements of Higgs boson properties are a complementary way to search for SUSY. Possible deviations of Higgs boson couplings from their SM values have been examined for natural SUSY in Refs. [35,36] and generally found to be substantial only for  $m_A \lesssim 0.75$ –1 TeV, or for relatively light stops [37,38] (which are either incompatible with current LHC limits or show near degeneracy with the LSP).

projected integrated luminosity (IL) of 15 ab<sup>-1</sup>. In Sec. III, we examine the four natural SUSY models introduced earlier and present LHC bounds in each of these search channels, and also obtain reach projections for HL- and HE-LHC. We find that while HL-LHC can probe a portion of natural SUSY parameter space, it will take an energy upgrade to the HE-LHC option for a definitive search for natural weak scale SUSY. In Sec. IV, we present a summary and conclusions. For some recent related work, see Refs. [46].

## II. UPDATED REACH PROJECTIONS OF HE-LHC FOR GLUINOS AND TOP SQUARKS

In this section, we update previous HE-LHC reach analyses for top-squark pair production [47] and gluino pair production [47,48] in natural SUSY, which were performed assuming  $\sqrt{s} = 33$  TeV and IL = 0.3–3 ab<sup>-1</sup> to the updated values assigned for the European Strategy report, namely  $\sqrt{s} = 27$  TeV and IL = 15 ab<sup>-1</sup>. Along these lines, our first step is to generate updated total production cross sections for our signal processes.

In Fig. 1, we plot the total production cross section for  $pp \rightarrow \tilde{g}\tilde{g}X$  (black) and  $pp \rightarrow \tilde{t}_1\tilde{t}_1^*X$  (orange) at both  $\sqrt{s} = 14$  (thin solid) and 27 TeV (thick solid). The results are computed at NLL + NLO and the 14 TeV results are taken from the study of Ref. [49] where we use the gluino pair

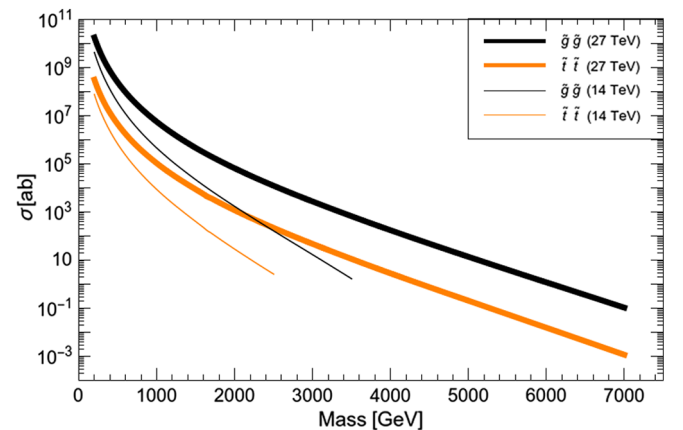


FIG. 1. Plot of NLL + NLO predictions [49] of  $\sigma(pp \rightarrow \tilde{g}\tilde{g}X)$  and  $\sigma(pp \rightarrow \tilde{t}_1\tilde{t}_1^*X)$  production at LHC for  $\sqrt{s} = 14$  and 27 TeV.



production results for decoupled squarks. Since Ref. [49] presents results for  $\sqrt{s} = 13, 14, 33$  and  $100$  TeV, we obtain total cross sections for  $\sqrt{s} = 27$  TeV via interpolation of the 14 and 33 TeV results. Specifically, we fit  $\log \sqrt{s}$  versus  $\log \sigma_{\text{tot}}$  to a quadratic and used the resulting function to obtain  $\sqrt{s} = 27$  TeV cross sections.

From the results shown in Fig. 1, we see that for  $m_{\tilde{g}} = 2$  TeV, the gluino pair production cross section ratio  $\sigma(27)/\sigma(14) = 38$  while for  $m_{\tilde{g}} = 3.5$  TeV this ratio increases to  $\sim 394$ . For  $m_{\tilde{t}} = 1$  TeV, we find a total top squark pair production ratio  $\sigma(27)/\sigma(14) = 12$  while for  $m_{\tilde{t}_1} = 2.5$  TeV  $\sigma(27)/\sigma(14)$  increases to 83. These ratios clearly reflect the advantage of moving to higher LHC energies in order to probe more massive strongly interacting sparticles.

### A. Updated top squark analysis for $\sqrt{s} = 27$ TeV

In Ref. [47], the reach of a 33 TeV LHC upgrade for top squark pair production was investigated. Here, we repeat the analysis but for updated LHC energy upgrade  $\sqrt{s} = 27$  TeV. We use Madgraph [50] to generate top squark pair production events within a simplified model where  $\tilde{t}_1 \rightarrow b\tilde{W}_1^+$  at 50%, and  $\tilde{t}_1 \rightarrow t\tilde{Z}_{1,2}$  each at 25% branching fraction, which are typical of most natural SUSY models [40]. The Higgsino-like electroweakino masses are  $m_{\tilde{Z}_{1,2}, \tilde{W}_1^\pm} \simeq 150$  GeV. We interface Madgraph with Pythia [51] for initial/final state showering, hadronization and underlying event simulation. The Delphes toy detector simulation [52] is used with specifications as listed in Ref. [47] (which we do not repeat here). We also used Madgraph-Pythia-Delphes for a variety of SM background processes that are listed in Table II.

In Ref. [47], an optimized set of cuts was found for extracting the signal from a 2.75 TeV top squark over SM backgrounds at  $\sqrt{s} = 33$  TeV LHC upgrade. The cuts that were settled upon were

- (i)  $n(b - \text{jets}) \geq 2$ ,
- (ii)  $n(\text{isol.leptons}) = 0$ ,
- (iii)  $E_T^{\text{miss}} > \max(1500 \text{ GeV}, 0.2M_{\text{eff}})$ ,
- (iv)  $E_T(j_1) > 1000$  GeV,
- (v)  $E_T(j_2) > 600$  GeV,

TABLE II. Cross sections in  $ab$  after cuts, listed in Sec. II A, from SM background processes for the top squark pair production analysis at  $\sqrt{s} = 27$  TeV.

Process	$\sigma$ (ab)
$b\bar{b}Z$	1.87
$t\bar{t}Z$	1.1
$t$	$4.4 \times 10^{-2}$
$t\bar{t}$	$3.3 \times 10^{-2}$
$t\bar{t}b\bar{b}$	$2.3 \times 10^{-2}$
$t\bar{t}t\bar{t}$	$1.7 \times 10^{-3}$
$t\bar{t}h$	$6.8 \times 10^{-4}$
total	3.07

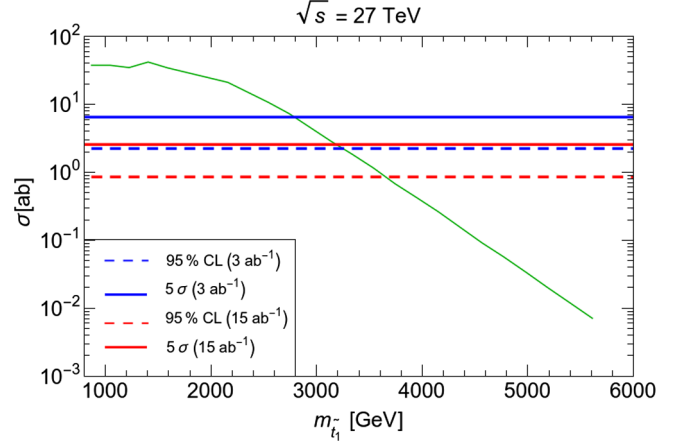


FIG. 2. Plot of top squark pair production cross section vs  $m_{\tilde{t}_1}$  after cuts at HE-LHC with  $\sqrt{s} = 27$  TeV (green curve). We also show the  $5\sigma$  and 95% CL reach lines assuming 3 and  $15 \text{ ab}^{-1}$  of integrated luminosity (for a single detector).

- (vi)  $S_T > 0.1$  and
- (vii)  $\Delta\phi(\vec{E}_T^{\text{miss}}, \text{jet close}) > 30$  deg.

In the above,  $M_{\text{eff}}$  is the usual effective mass variable,  $S_T$  is transverse sphericity and the  $\Delta\phi$  cut is on the transverse opening angle between the missing  $E_T$  vector and the closest jet (which helps reduce background from boosted tops in  $t\bar{t}$  production). The surviving background rates in  $ab$  are listed in Table II. We use the same  $K$ -factors as listed in Ref. [47] to bring our total background cross sections into accord with various beyond-leading-order calculations. In the present analysis, we have also included the  $t\bar{t}Z$  background calculation, which was not present in Ref. [47].

Using these background rates for the LHC at  $\sqrt{s} = 27$  TeV, we compute the  $5\sigma$  and 95% CL reach of HE-LHC for 3 and  $15 \text{ ab}^{-1}$  of integrated luminosity using Poisson statistics. These results are plotted in Fig. 2 along with the top squark pair production cross section after cuts versus  $m_{\tilde{t}_1}$ . From the figure, we see the  $5\sigma$  discovery reach of LHC27 extends to  $m_{\tilde{t}_1} = 2800$  GeV for  $3 \text{ ab}^{-1}$  and to 3160 GeV for  $15 \text{ ab}^{-1}$ . The 95% CL exclusion limits extend to  $m_{\tilde{t}_1} = 3250$  GeV for  $3 \text{ ab}^{-1}$  and to  $m_{\tilde{t}_1} = 3650$  GeV for  $15 \text{ ab}^{-1}$ . We see that  $S/B$  exceeds 0.8 whenever we deem the signal to be observable. Of course, somewhat increased reach limits can be obtained in the event of a combined ATLAS/CMS analysis.<sup>5</sup>

<sup>5</sup>The reader may wonder whether the stop reach would be significantly enhanced if the lighter stop was mainly left-handed so that the signal also receives comparable contributions from sbottom pair production. We view a significant increase in the signal rate to be unlikely in high scale models because even if the  $LL$  diagonal elements of the stop and sbottom squared mass matrices are comparable, the much larger off-diagonal element of the stop mass squared matrix will tend to depress the mass of  $\tilde{t}_1$  to be well below that of  $\tilde{b}_1$ . The reader may view the reach projection in the figure as only slightly erring on the conservative side. For related discussion, see e.g., Refs. [53,54].

TABLE III. Cross sections in  $ab$  after cuts, listed in Sec. II B, from SM background processes for the gluino pair production analysis at  $\sqrt{s} = 27$  TeV.

Process	$\sigma$ (ab)
$b\bar{b}Z$	0.061
$t\bar{t}Z$	0.037
$t$	0.003
$\bar{t}$	0.026
$\bar{t}b\bar{b}$	0.0046
$\bar{t}t\bar{t}$	0.0
$\bar{t}th$	$8.1 \times 10^{-4}$
total	0.132

### B. Updated gluino analysis for $\sqrt{s} = 27$ TeV

In Ref. [47], optimized cuts were investigated for extracting the signal from a 5.4 TeV gluino over SM backgrounds at a  $\sqrt{s} = 33$  TeV LHC upgrade. The optimized cuts were found to be

- (i)  $n(b - \text{jets}) \geq 2$ ,
- (ii)  $n(\text{isol.leptons}) = 0$ ,
- (iii)  $E_T^{\text{miss}} > \max(1900 \text{ GeV}, 0.2M_{\text{eff}})$ ,
- (iv)  $E_T(j_1) > 1300 \text{ GeV}$ ,
- (v)  $E_T(j_2) > 900 \text{ GeV}$ ,
- (vi)  $E_T(j_3) > 200 \text{ GeV}$ ,
- (vii)  $E_T(j_4) > 200 \text{ GeV}$ ,
- (viii)  $S_T > 0.1$  and
- (ix)  $\Delta\phi(\vec{E}_T^{\text{miss}}, \text{jet close}) > 10 \text{ deg.}$

The corresponding backgrounds in  $ab$  after cuts are listed in Table III. The backgrounds are again normalized to recent beyond-leading-order results as detailed in Ref. [47]. We again compute the  $5\sigma$  reach and 95% CL exclusion lines using Poisson statistics for 3 and 15  $\text{ab}^{-1}$  of integrated luminosity.

Our results are shown in Fig. 3 where we plot the gluino pair production signal versus  $m_{\tilde{g}}$  for a nNUHM2 model line

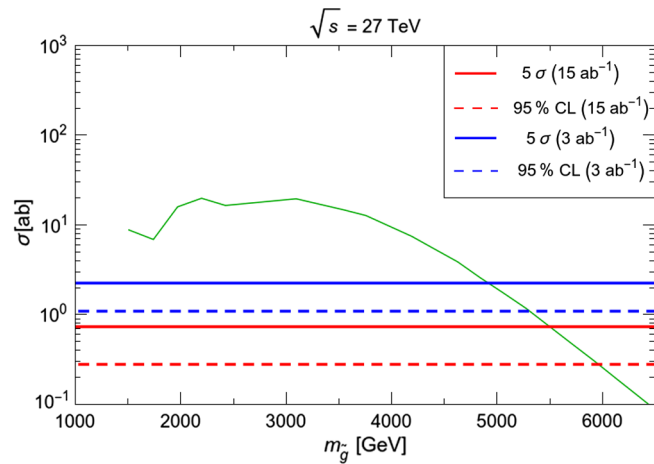


FIG. 3. Plot of gluino pair production cross section vs  $m_{\tilde{g}}$  after cuts at HE-LHC with  $\sqrt{s} = 27$  TeV (green curve). We also show the  $5\sigma$  and 95% CL reach lines assuming 3 and 15  $\text{ab}^{-1}$  of integrated luminosity.

with parameter choice  $m_0 = 5m_{1/2}$ ,  $A_0 = -1.6m_0$ ,  $m_A = m_{1/2}$ ,  $\tan\beta = 10$  and  $\mu = 150$  GeV with varying  $m_{1/2}$ . We do not expect the results to be sensitive to this precise choice as long as first generation squarks are heavy. From the figure, we see that the  $5\sigma$  discovery reach of LHC27 extends to  $m_{\tilde{g}} = 4900$  GeV for 3  $\text{ab}^{-1}$  and to  $m_{\tilde{g}} = 5500$  GeV for 15  $\text{ab}^{-1}$  of integrated luminosity. The corresponding 95% CL exclusion reaches extend to  $m_{\tilde{g}} = 5300$  GeV for 3  $\text{ab}^{-1}$  and to  $m_{\tilde{g}} = 5900$  GeV for 15  $\text{ab}^{-1}$  of integrated luminosity.<sup>6</sup>

## III. CONFRONTING NATURAL SUSY MODELS AT THE LHC AND ITS UPGRADES

### A. Gluino pair production

In Fig. 4 we display the results of our scans over parameter space of the nNUMH2, nNUHM3, nAMSB and nGMM models with  $\Delta_{\text{EW}} < 30$  and with  $m_h$ : 123–127 GeV in the  $m_{\tilde{g}}$  vs  $m_{\tilde{Z}_1}$  plane. We also require  $m_{\tilde{g}} > 2$  TeV and  $m_{\tilde{t}_1} > 1.1$  TeV in accord with recent simplified model mass limits from ATLAS and CMS. The density of points is not to be taken as meaningful. Indeed, in a statistical study of IIB string theory landscape [55], it is argued that there should exist a power law draw to large soft terms that would not be reflected here but that would then favor larger sparticle masses beyond current LHC reach and  $m_h \simeq 125$  GeV. The available natural parameter space can be construed as some boundary enclosing all the natural SUSY scan points in accord with the measured Higgs mass and current LHC sparticle mass constraints.

From Fig. 4, we see that the range of  $m_{\tilde{g}}$  extends from about 2 TeV to around  $m_{\tilde{g}} \sim 6$  TeV for NUHM2,3 and nGMM models but to significantly higher values for nAMSB. The upper limit on  $m_{\tilde{g}}$  occurs because the gluino mass drives top squark soft mass terms to such large values that  $\Sigma_{\tilde{t}}^u(\tilde{t}_{1,2}) > 30$ , leading to a violation of our naturalness criterion. To understand why higher gluino masses are allowed in the nAMSB model, we first note that  $m_{\tilde{g}} \gtrsim 6$  TeV occurs only for *negative* values of  $A_0$ . In this case, in order to obtain  $m_h$  consistent with its observed value very large negative magnitudes of  $A_0$  are required (compared to the positive  $A_0$  case). The resulting very large contribution of  $A_t$  to their renormalization group evolution then strongly suppresses the weak scale soft top squark mass parameters, allowing correspondingly larger values of  $m_{\tilde{g}}$  (*vis à vis* the other models). The fact that  $|M_2|$  is smaller than  $|M_3|$  in the nAMSB case also helps. The range of  $m_{\tilde{Z}_1}$  varies from

<sup>6</sup>For third generation squarks heavier than the gluino, Fig. 11 of Ref. [47] shows that the gluino reach is independent of the composition of  $\tilde{t}_1$ . If the stop is much lighter than the gluino, stop production may add a subdominant contribution to the gluino event sample as shown in Fig. 12 of Ref. [47]. For our assessment of the HE-LHC reach, we have conservatively assumed the signal comes only from gluino pair production.

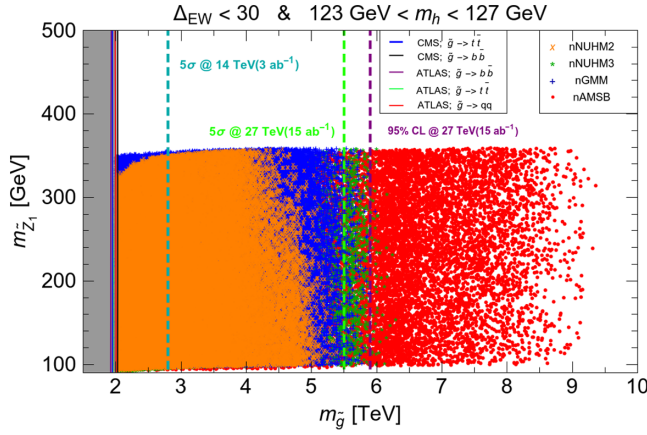


FIG. 4. Plot of points in the  $m_{\tilde{g}}$  vs  $m_{\tilde{Z}_1}$  plane from a scan over nNUHM2, nNUHM3, nGMM and nAMSMB model parameter space. We compare to recent search limits from the ATLAS/CMS experiments (solid vertical lines) and future LHC upgrade options (dashed vertical lines).

100–350 GeV in accord with the range of  $\mu$  that is bounded from below by LEP2 searches for chargino pair production and bounded from above by naturalness in Eq. (3). We also show by the solid vertical lines around  $m_{\tilde{g}} \sim 2$  TeV the results of several ATLAS and CMS simplified model search limits for gluino pair production [12,13]. It is apparent from the plot that a large range of parameter space remains to be explored. The blue dashed line around  $m_{\tilde{g}} \sim 2800$  GeV shows the computed  $5\sigma$  reach of high luminosity LHC (HL-LHC) with  $\sqrt{s} = 14$  TeV and  $3 \text{ ab}^{-1}$  of integrated luminosity [56]. While the HL-LHC will somewhat extend the SUSY search via the gluino pair production channel, much of the allowed gluino mass range will remain beyond its reach. We also show with the green (purple) dashed lines the HE-LHC  $5\sigma$  reach (95% CL exclusion region) for gluino pair production as computed in Sec. II for  $\sqrt{s} = 27$  TeV and  $15 \text{ ab}^{-1}$  of IL. We see that HE-LHC should probe nearly all of parameter space for the nNUHM2, nNUHM3 and nGMM models while evidently a considerable fraction of nAMSMB parameter space would be beyond HE-LHC reach in the gluino pair production channel.

### B. Top squark pair production

In Fig. 5, we show the locus of scan points from the four natural SUSY models in the  $m_{\tilde{t}_1}$  vs  $m_{\tilde{Z}_1}$  plane. The  $m_{\tilde{Z}_1}$  value is bounded by  $\sim 350$  GeV so almost no points occupy the near degeneracy region  $m_{\tilde{t}_1} \sim m_{\tilde{Z}_1}$  where much LHC search effort has focused. We also show the current search limits from ATLAS [14] and CMS [15] as solid red and black contours, respectively. These LHC search limits exclude some of natural SUSY parameter space but evidently a large swath of natural SUSY parameter space remains to be explored since top squark masses may extend up to  $m_{\tilde{t}_1} \sim 3.5$  TeV without compromising naturalness.

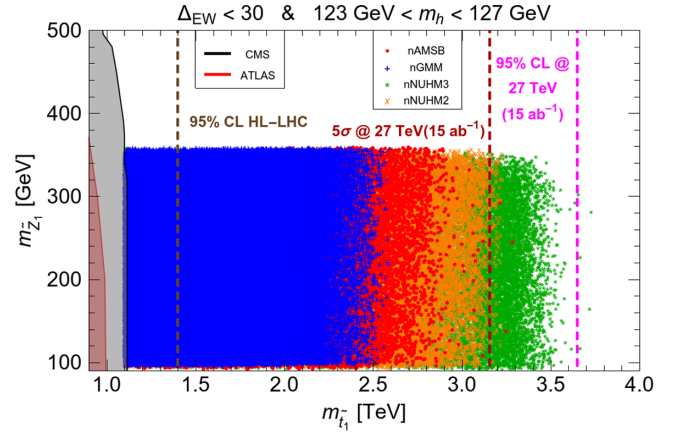


FIG. 5. Plot of points in the  $m_{\tilde{t}_1}$  vs  $m_{\tilde{Z}_1}$  plane from a scan over nNUHM2, nNUHM3, nGMM and nAMSMB model parameter space. We compare to recent search limits from the ATLAS/CMS experiments (solid contours) and to projected future limits (dashed lines).

The ATLAS collaboration projected 95% CL exclusion region for top squarks at HL-LHC [57] is also shown by the black dashed line at  $m_{\tilde{t}_1} \sim 1.4$  TeV. While HL-LHC will probe additional parameter space, much of the top squark mass range will lie beyond its reach. The reach of HE-LHC with  $\sqrt{s} = 27$  TeV and IL of  $15 \text{ ab}^{-1}$  was computed in Sec. II. We show the  $5\sigma$  reach contour as a red dashed line extending out to  $m_{\tilde{t}_1} \sim 3.1$  TeV while the 95% CL exclusion region extends to  $m_{\tilde{t}_1} \sim 3650$  GeV. The HE-LHC apparently will be able to probe essentially the entire natural SUSY parameter space in the top squark pair production channel.

In Fig. 6 we show the gluino and top squark reach values in the  $m_{\tilde{t}_1}$  vs  $m_{\tilde{g}}$  plane. The gray shaded region is excluded by the current search limits from CMS [13,15]. In this plane, it is important to note that in the nNUHM2, nNUHM3 and nGMM models, the highest values of  $m_{\tilde{g}}$

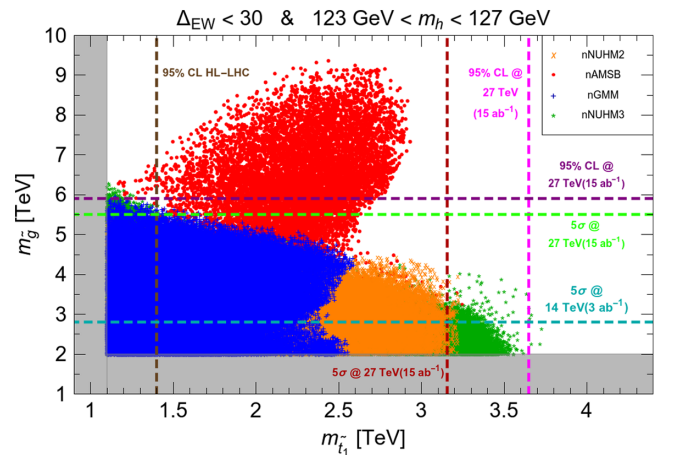


FIG. 6. Plot of points in the  $m_{\tilde{t}_1}$  vs  $m_{\tilde{g}}$  plane from a scan over nNUHM2, nNUHM3, nGMM and nAMSMB model parameter space. We compare to projected future search limits from the LHC experiments.



correspond to the lowest values of  $m_{\tilde{t}_1}$  while the highest  $m_{\tilde{t}_1}$  values correspond to the lowest  $m_{\tilde{g}}$  values. Thus, a marginal signal in one of these channels (due to sparticle masses being near their upper limit) should correspond to a robust signal in the complementary channel. In particular, for nNUHM3 where gluinos might be slightly beyond HE-LHC reach, the top squarks should be readily detectable. The nAMSB model case is different, because as we saw in Sec. III A, the very large negative values of  $A_0$  needed to obtain the correct value of  $m_h$  allow gluino masses in the 6–9 TeV range with modest values of  $m_{\tilde{t}_1}$ . (The top squark and gluino mass values in the nAMSB model with  $A_0 > 0$  are in line with those in the other models.) We see that while gluino pair production might escape detection at the HE-LHC in the nAMSB framework, the top squark signal should be easily visible since  $m_{\tilde{t}_1} \lesssim 3$  TeV in this case.

### C. Higgsino pair production

The four Higgsino-like neutralinos  $\tilde{W}_1^\pm$  and  $\tilde{Z}_{1,2}$  are the only SUSY particles required by naturalness to lie not too far above the weak scale,  $m_{\text{weak}} \sim 100$  GeV. In spite of their lightness, they are very challenging to detect at the LHC. The lightest neutralino evidently comprises only a subdominant part of dark matter [58] and if produced at LHC via  $pp \rightarrow \tilde{Z}_1 \tilde{Z}_1$  would escape detection. In fact, signals from electroweak Higgsino pair production  $pp \rightarrow \tilde{Z}_i \tilde{Z}_j$ ,  $\tilde{W}_1 \tilde{Z}_i$ ,  $\tilde{W}_1 \tilde{W}_1 + X$  ( $i, j = 1, 2$ ) are undetectable above SM backgrounds such as vector boson and top quark pair production because the decay products of the heavier Higgsinos  $\tilde{W}_1$  and  $\tilde{Z}_2$  are expected to be soft. The monojet signal arising from initial state QCD radiation in Higgsino pair production events has been evaluated in Ref. [41] and was found to have similar shape distributions to the dominant  $pp \rightarrow Zj$  background but with background levels about 100 times larger than signal. See, however, Ref. [59].

A way forward has been proposed via the  $pp \rightarrow \tilde{Z}_1 \tilde{Z}_2 j$  channel where  $\tilde{Z}_2 \rightarrow \ell^+ \ell^- \tilde{Z}_1$ : a soft opposite-sign (OS) dilepton pair recoils against a hard initial state jet radiation, which serves as a trigger [42]. Recent searches in this  $\ell^+ \ell^- j + \cancel{E}_T$  channel have been performed by CMS [43] and by ATLAS [44]. Their resultant reach contours are shown as solid black and blue contours respectively in the  $m_{\tilde{Z}_2}$  vs  $m_{\tilde{Z}_2} - m_{\tilde{Z}_1}$  plane in Fig. 7. These searches have indeed begun to probe the most promising portion of the parameter space, since the lighter range of  $m_{\tilde{Z}_2}$  masses have some preference from naturalness. The CMS experiment has also presented projected exclusion contours for LHC14 with  $300 \text{ fb}^{-1}$  and HL-LHC with  $3 \text{ ab}^{-1}$  shown as the green and purple dashed contours [60]. We see that while these contours can probe considerably more parameter space, much of natural SUSY parameter space lies beyond these projected reaches. So far, reach contours for HE-LHC in this search channel have not been computed but it may be

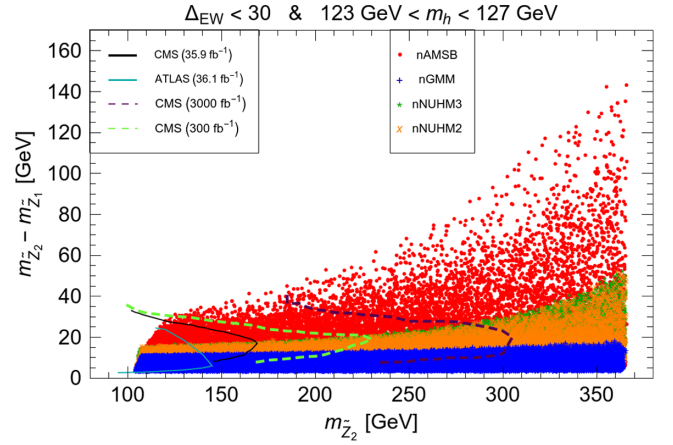


FIG. 7. Plot of points in the  $m_{\tilde{Z}_2}$  vs  $m_{\tilde{Z}_2} - m_{\tilde{Z}_1}$  plane from a scan over nNUHM2, nNUHM3, nGMM and nAMSB model parameter space. We compare to recent search limits from the ATLAS/CMS experiments and some projected luminosity upgrades as computed by CMS.

anticipated that HE-LHC will not be greatly beneficial here since  $pp \rightarrow \tilde{Z}_1 \tilde{Z}_2 j + X$  is primarily an electroweak production process so the signal cross section will increase only marginally while QCD background processes like  $t\bar{t}$  production will increase substantially: harder cuts may, however, be possible. The nAMSB model inhabits typically a larger mass gap region of the plane since in this model winos are much lighter than in nNUHM2 or nGMM for a given gluino mass. It is imperative that future LHC searches try to squeeze their reach to the lowest  $m_{\tilde{Z}_2} - m_{\tilde{Z}_1}$  mass gaps, which are favored to lie in the 3–5 GeV region for string landscape projections [55].

### D. Wino pair production

The wino pair production reaction  $pp \rightarrow \tilde{W}_2^\pm \tilde{Z}_4 X$  (in nNUHM2,3 and nGMM) or  $pp \rightarrow \tilde{W}_2^\pm \tilde{Z}_3 X$  (in nAMSB) offers a new and lucrative search channel that is not present in unnatural models where  $|\mu| \gg M_{\text{gauginos}}$ . The decay modes  $\tilde{W}_2^\pm \rightarrow W^\pm \tilde{Z}_{1,2}$  and  $\tilde{Z}_3 \text{ or } 4 \rightarrow W^\pm \tilde{W}_1^\mp$  lead to a SSdB plus  $\cancel{E}_T$  final states accompanied by minimal jet activity—just that arising from initial state radiation [45]. Thus, the ensuing same-sign dilepton+ $\cancel{E}_T$  signature is quite different from that which arises from gluino and squark pair production where multiple hard jets are expected to be present. The SSdB signature from wino pair production has very low SM backgrounds that might arise from processes like  $t\bar{t}W$  production.<sup>7</sup>

<sup>7</sup>Of course, an OS dilepton +  $\cancel{E}_T$  signature also emerges from wino pair production at comparable rates to SSdB production. However, the OS dilepton signal channel has huge backgrounds from SM processes like  $W^+W^-$  and  $ZZ \rightarrow \tau + \tau \nu \nu$  production. Thus, we expect that LHC experiments will have a far greater reach for natural SUSY in the SSdB signal channel.



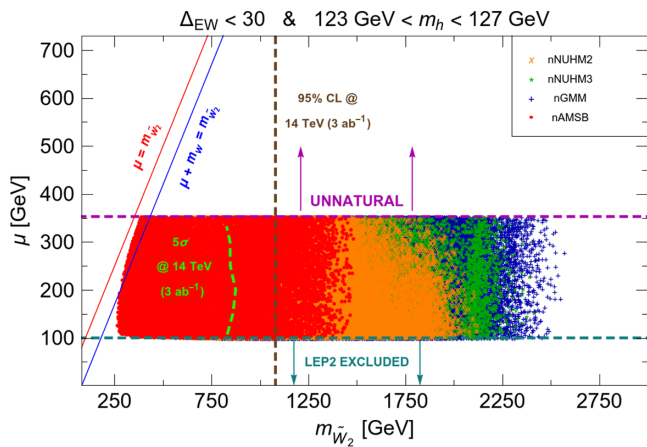


FIG. 8. Plot of points in the  $m_{\tilde{W}_2}$  vs  $\mu$  plane from a scan over nNUHM2, nNUHM3, nGMM and nAMSB model parameter space. We compare to projected search limits for the ATLAS/CMS experiments at HL-LHC.

In Fig. 8 we show the location of natural SUSY model points in the  $m_{\tilde{W}_2}$  vs  $\mu$  plane. The region with large  $\mu$  is increasingly unnatural as indicated in the plot. From Fig. 8, we see that the nAMSB model points tend to populate the lower  $m_{\tilde{W}_2}$  region,  $m_{\tilde{W}_2} \lesssim 1400$  GeV. This is because  $M_2 \sim m_{\tilde{g}}/7$  in AMSB models with  $m_{\tilde{g}} \lesssim 6-9$  TeV from naturalness considerations.

We are unaware of any LHC search limits via the SSdB channel, though this signature should begin to be competitive with the conventional  $\cancel{E}_T$  searches for an integrated luminosity of  $\sim 100 \text{ fb}^{-1}$  expected to be accumulated by the end of LHC Run 2. The projected HL-LHC reach has been evaluated in Ref. [45] where the  $5\sigma$  discovery and 95% CL exclusion dashed contours are shown. Evidently HL-LHC will be able to probe a large part of parameter space for the nAMSB model while only a lesser portion of natural parameter space of nNUHM2, nNUHM3 and nGMM models can be probed. The corresponding reach of HE-LHC has not been computed for the SSdB channel. But again, since this is an EW production channel, the signal rates are expected to rise by a factor of a few by moving from  $\sqrt{s} = 14$  TeV to  $\sqrt{s} = 27$  TeV while some of the QCD backgrounds like  $t\bar{t}$  production will rise by much larger factors. We also note that because the heavy winos are expected to decay to Higgsinos plus a  $W^\pm$ ,  $Z$  or  $h$  in the ratio 2:1:1 [45],  $VV$ ,  $Vh$  and  $hh$  plus  $\cancel{E}_T$  signals may be present, possibly with additional soft leptons from Higgsino decays. A study of these signals is beyond the scope of the present analysis.

#### IV. SUMMARY AND CONCLUSIONS

Our goal, in this paper, was to ascertain what sort of LHC upgrades might be sufficient to either discover or falsify natural supersymmetry. We focused here on natural SUSY

spectra consistent with the measured value of the weak scale  $m_{\text{weak}} \sim 100$  GeV without a need for implausible fine-tuning of model parameters. Naturalness, after all, remains one of the major motivations for weak supersymmetry and unnatural models seem highly implausible. To this end, we scanned over four different natural SUSY models: nNUHM2, nNUHM3, nAMSB and nGMM. We obtained upper limits on top squark masses ( $m_{\tilde{t}_1} \lesssim 3.5$  TeV), gluino masses ( $m_{\tilde{g}} \lesssim 6$  TeV in nNUHM2,3 and nGMM, but  $m_{\tilde{g}} \lesssim 9$  TeV in nAMSB) and Higgsino and wino masses.

We compared these against current LHC constraints and found large regions of natural SUSY parameter space remain to be explored. We also compared against the HL-LHC upgrade: the HL-LHC with  $\sqrt{s} = 14$  TeV and  $3 \text{ ab}^{-1}$  of integrated luminosity will explore deeper into natural SUSY parameter space but, barring a SUSY discovery, much of the parameter space will remain to be explored. We also updated the HE-LHC reach using the revised energy and integrated luminosity targets as suggested by the ongoing European Strategy study:  $\sqrt{s} = 27$  TeV and  $IL = 15 \text{ ab}^{-1}$ . For these latter values, we find a HE-LHC reach in  $m_{\tilde{t}_1}$  to 3200 GeV at  $5\sigma$  and 3650 GeV at 95% CL. For the gluino, we find a HE-LHC reach to  $m_{\tilde{g}} = 5500$  GeV at  $5\sigma$  and 6000 GeV at 95% CL. The gluino (top squark) reach is reduced by about 600 GeV (400 GeV) if the integrated luminosity is instead  $3 \text{ ab}^{-1}$ .

Comparing these values with upper limits from naturalness, we find the HE-LHC is sufficient to probe the entire natural SUSY parameter space in the top squark pair production channel and also to almost explore nNUHM2,3 and nGMM models in the gluino pair channel. Within these models it is, therefore, very likely that signals from top squark and gluino pair production will be present at the HE-LHC. In the nAMSB model, it appears that gluinos may be beyond the HE-LHC reach.

We also compared the soft OS dilepton + jet signal from Higgsino pair production to current and future reach projections for HL-LHC. For this channel, it will be important to explore neutralino mass gaps  $m_{\tilde{Z}_2} - m_{\tilde{Z}_1}$  down to  $\sim 3$  GeV and Higgsino masses up to  $\sim 350$  GeV for complete coverage. We caution that the energy upgrade of the LHC may not be as beneficial for this discovery channel since QCD backgrounds are expected to rise more rapidly with energy than the EW Higgsino pair production signal channel. We also examined the SSdB signature arising from charged and neutral wino pair production. The HL-LHC may explore a portion of—but not all of—natural SUSY parameter space in this channel. It is again unclear whether an energy upgrade will help much in this channel since QCD backgrounds are expected to increase more rapidly than the electroweak (EW)-produced signal channel for an assumed wino mass  $m_{\tilde{W}_2}$ . We note, though, that there may be signals from wino pair production in  $VV$ ,  $Vh$  and  $hh + \cancel{E}_T$  channels that may also be interesting to explore.

To sum up: the key theoretical motivation for *weak scale* supersymmetry as the stabilizer of the Higgs sector still remains, once we acknowledge that model parameters that are usually taken to be independent in spectra computer codes are expected to be correlated in any ultraviolet complete theory. Our final assessment is that the search for natural SUSY will, and should, continue on at LHC and HL-LHC, where more extensive regions of parameter space may be explored. The envisioned HE-LHC upgrade to  $\sqrt{s} = 27$  TeV and  $\text{IL} = 15 \text{ ab}^{-1}$  seems sufficient to either discover or falsify natural SUSY in the top squark pair production signal channel, very possibly with an additional signal in the gluino-pair production channel. It is possible

that observable signals may also emerge in the wino-pair or Higgsino-pair plus monojet search channels as well.

## ACKNOWLEDGMENTS

This work was supported in part by the U.S. Department of Energy, Office of High Energy Physics. The computing for this project was performed at the OU Supercomputing Center for Education & Research (OSCER) at the University of Oklahoma (OU). X.T. thanks the Centre for High Energy Physics, Indian Institute of Science Bangalore, where part of this work was done for their hospitality, and also the Infosys Foundation for financial support that made his visit to Bangalore possible.

- 
- [1] G. Aad *et al.* (ATLAS Collaboration), *Phys. Lett. B* **716**, 1 (2012); S. Chatrchyan *et al.* (CMS Collaboration), *Phys. Lett. B* **716**, 30 (2012).
- [2] M. J. G. Veltman, *Acta Phys. Pol. B* **12**, 437 (1981).
- [3] M. Einhorn and D. R. T. Jones, *Phys. Rev. D* **46**, 5206 (1992).
- [4] The ATLAS Collaboration, Report No. ATLAS-CONF-2017-046; G. Aad *et al.* (ATLAS and CMS Collaborations), *Phys. Rev. Lett.* **114**, 191803 (2015).
- [5] E. Witten, *Nucl. Phys.* **B188**, 513 (1981); R. K. Kaul, *Phys. Lett.* **109B**, 19 (1982).
- [6] H. Baer and X. Tata, *Weak Scale Supersymmetry: From Superfields to Scattering Events* (Cambridge University Press, Cambridge, 2006), p. 537.
- [7] S. Dimopoulos, S. Raby, and F. Wilczek, *Phys. Rev. D* **24**, 1681 (1981).
- [8] J. R. Ellis, S. Kelley, and D. V. Nanopoulos, *Phys. Lett. B* **260**, 131 (1991); U. Amaldi, W. de Boer, and H. Furstenau, *Phys. Lett. B* **260**, 447 (1991); P. Langacker and M. x. Luo, *Phys. Rev. D* **44**, 817 (1991).
- [9] L. E. Ibañez and G. G. Ross, *Phys. Lett.* **110B**, 215 (1982); K. Inoue, A. Kakuto, H. Komatsu, and S. Takeshita, *Prog. Theor. Phys.* **68**, 927 (1982); **71**, 413 (1984); L. Ibañez, *Phys. Lett.* **118B**, 73 (1982); H. P. Nilles, M. Srednicki, and D. Wyler, *Phys. Lett.* **120B**, 346 (1983); J. Ellis, J. Hagelin, D. Nanopoulos, and M. Tamvakis, *Phys. Lett.* **125B**, 275 (1983); L. Alvarez-Gaumé, J. Polchinski, and M. Wise, *Nucl. Phys.* **B221**, 495 (1983); B. A. Ovrut and S. Raby, *Phys. Lett.* **130B**, 277 (1983); for a review, see L. E. Ibanez and G. G. Ross, *C.R. Phys.* **8**, 1013 (2007).
- [10] M. S. Carena and H. E. Haber, *Prog. Part. Nucl. Phys.* **50**, 63 (2003).
- [11] H. Baer, V. Barger, and A. Mustafayev, *Phys. Rev. D* **85**, 075010 (2012); A. Arbey, M. Battaglia, A. Djouadi, F. Mahmoudi, and J. Quevillon, *Phys. Lett. B* **708**, 162 (2012); L. J. Hall, D. Pinner, and J. T. Ruderman, *J. High Energy Phys.* **04** (2012) 131.
- [12] The ATLAS Collaboration, Report No. ATLAS-CONF-2017-022.
- [13] A. M. Sirunyan *et al.* (CMS Collaboration), *Phys. Rev. D* **97**, 012007 (2018); *Eur. Phys. J. C* **77**, 710 (2017).
- [14] The ATLAS Collaboration, Report No. ATLAS-CONF-2017-037.
- [15] A. M. Sirunyan *et al.* (CMS Collaboration), *J. High Energy Phys.* **10** (2017) 019.
- [16] J. Ellis, K. Enqvist, D. Nanopoulos, and F. Zwirner, *Mod. Phys. Lett. A* **01**, 57 (1986); R. Barbieri and G. Giudice, *Nucl. Phys.* **B306**, 63 (1988).
- [17] G. W. Anderson and D. J. Castano, *Phys. Rev. D* **52**, 1693 (1995).
- [18] S. Dimopoulos and G. F. Giudice, *Phys. Lett. B* **357**, 573 (1995).
- [19] R. Kitano and Y. Nomura, *Phys. Rev. D* **73**, 095004 (2006); M. Papucci, J. T. Ruderman, and A. Weiler, *J. High Energy Phys.* **09** (2012) 035; C. Brust, A. Katz, S. Lawrence, and R. Sundrum, *J. High Energy Phys.* **03** (2012) 103.
- [20] H. Baer, V. Barger, and D. Mickelson, *Phys. Rev. D* **88**, 095013 (2013).
- [21] A. Mustafayev and X. Tata, *Indian J. Phys.* **88**, 991 (2014).
- [22] H. Baer, V. Barger, D. Mickelson, and M. Padeffke-Kirkland, *Phys. Rev. D* **89**, 115019 (2014).
- [23] H. Baer, V. Barger, P. Huang, A. Mustafayev, and X. Tata, *Phys. Rev. Lett.* **109**, 161802 (2012).
- [24] H. Baer, V. Barger, P. Huang, D. Mickelson, A. Mustafayev, and X. Tata, *Phys. Rev. D* **87**, 115028 (2013).
- [25] H. Baer, V. Barger, and M. Savoy, *Phys. Rev. D* **93**, 035016 (2016).
- [26] K. L. Chan, U. Chattopadhyay, and P. Nath, *Phys. Rev. D* **58**, 096004 (1998).
- [27] H. Baer, V. Barger, and P. Huang, *J. High Energy Phys.* **11** (2011) 031.
- [28] D. Matalliotakis and H. P. Nilles, *Nucl. Phys.* **B435**, 115 (1995); M. Olechowski and S. Pokorski, *Phys. Lett. B* **344**, 201 (1995); P. Nath and R. L. Arnowitt, *Phys. Rev. D* **56**, 2820 (1997); J. Ellis, K. Olive, and Y. Santoso, *Phys. Lett. B* **539**, 107 (2002); J. Ellis, T. Falk, K. Olive, and Y. Santoso, *Nucl. Phys.* **B652**, 259 (2003); H. Baer, A. Mustafayev,

- S. Profumo, A. Belyaev, and X. Tata, *J. High Energy Phys.* **07** (2005) 065.
- [29] O. Lebedev, H. P. Nilles, S. Raby, S. Ramos-Sanchez, M. Ratz, P. K. S. Vaudrevange, and A. Wingerter, *Phys. Lett. B* **645**, 88 (2007); M. Badziak, S. Krippendorf, H. P. Nilles, and M. W. Winkler, *J. High Energy Phys.* **03** (2013) 094.
- [30] H. Baer, V. Barger, M. Savoy, H. Serce, and X. Tata, *J. High Energy Phys.* **06** (2017) 101.
- [31] L. Randall and R. Sundrum, *Nucl. Phys.* **B557**, 79 (1999); H. Baer, V. Barger, and D. Sengupta, *Phys. Rev. D* **98**, 015039 (2018).
- [32] K. Choi, A. Falkowski, H. P. Nilles, M. Olechowski, and S. Pokorski, *J. High Energy Phys.* **11** (2004) 076; K. Choi, A. Falkowski, H. P. Nilles, and M. Olechowski, *Nucl. Phys.* **B718**, 113 (2005); J. P. Conlon, F. Quevedo, and K. Suruliz, *J. High Energy Phys.* **08** (2005) 007; K. Choi, K.-S. Jeong, and K. Okumura, *J. High Energy Phys.* **09** (2005) 039.
- [33] H. Baer, V. Barger, H. Serce, and X. Tata, *Phys. Rev. D* **94**, 115017 (2016).
- [34] H. Baer, F. Paige, S. Protopopescu, and X. Tata, [arXiv:hep-ph/0312045](https://arxiv.org/abs/hep-ph/0312045); H. Baer, C. H. Chen, R. B. Munroe, F. E. Paige, and X. Tata, *Phys. Rev. D* **51**, 1046 (1995).
- [35] K. J. Bae, H. Baer, N. Nagata, and H. Serce, *Phys. Rev. D* **92**, 035006 (2015).
- [36] T. Li, S. Raza, and K. Wang, *Phys. Rev. D* **93**, 055040 (2016).
- [37] J. Fan and M. Reece, *J. High Energy Phys.* **06** (2014) 031.
- [38] A. Kobakhidze, N. Liu, L. Wu, J. M. Yang, and M. Zhang, *Phys. Lett. B* **755**, 76 (2016).
- [39] V. D. Barger, R. W. Robinett, W. Y. Keung, and R. J. N. Phillips, *Phys. Lett.* **131B**, 372 (1983); H. Baer, X. Tata, and J. Woodside, *Phys. Rev. D* **42**, 1568 (1990); H. Baer, C. h. Chen, M. Drees, F. Paige, and X. Tata, *Phys. Rev. D* **58**, 075008 (1998).
- [40] H. Baer, V. Barger, N. Nagata, and M. Savoy, *Phys. Rev. D* **95**, 055012 (2017).
- [41] H. Baer, A. Mustafayev, and X. Tata, *Phys. Rev. D* **89**, 055007 (2014); see also C. Han, A. Kobakhidze, N. Liu, A. Saavedra, L. Wu, and J. M. Yang, *J. High Energy Phys.* **02** (2014) 049; P. Schwaller and J. Zurita, *J. High Energy Phys.* **03** (2014) 060.
- [42] Z. Han, G. D. Kribs, A. Martin, and A. Menon, *Phys. Rev. D* **89**, 075007 (2014); H. Baer, A. Mustafayev, and X. Tata, *Phys. Rev. D* **90**, 115007 (2014); C. Han, D. Kim, S. Munir, and M. Park, *J. High Energy Phys.* **04** (2015) 132.
- [43] CMS Collaboration, Report No. CMS-PAS-SUS-16-048.
- [44] M. Aaboud *et al.* (ATLAS Collaboration), *Phys. Rev. D* **97**, 052010 (2018).
- [45] H. Baer, V. Barger, P. Huang, D. Mickelson, A. Mustafayev, W. Sreethawong, and X. Tata, *Phys. Rev. Lett.* **110**, 151801 (2013); *J. High Energy Phys.* **12** (2013) 013; **06** (2015) 53; H. Baer, V. Barger, J. S. Gainer, M. Savoy, D. Sengupta, and X. Tata, *Phys. Rev. D* **97**, 035012 (2018).
- [46] A. Aboubrahim and P. Nath, *Phys. Rev. D* **98**, 015009 (2018).
- [47] H. Baer, V. Barger, J. S. Gainer, H. Serce, and X. Tata, *Phys. Rev. D* **96**, 115008 (2017).
- [48] H. Baer, V. Barger, J. S. Gainer, P. Huang, M. Savoy, H. Serce, and X. Tata, *Phys. Lett. B* **774**, 451 (2017).
- [49] C. Borschensky, M. Krmer, A. Kulesza, M. Mangano, S. Padhi, T. Plehn, and X. Portell, *Eur. Phys. J. C* **74**, 3174 (2014).
- [50] J. Alwall, M. Herquet, F. Maltoni, O. Mattelaer, and T. Stelzer, *J. High Energy Phys.* **06** (2011) 128; J. Alwall, R. Frederix, S. Frixione, V. Herschi, F. Maltoni, O. Mattelaer, H.-S. Shao, T. Stelzer, P. Torrielli, and M. Zaro, *J. High Energy Phys.* **07** (2014) 079.
- [51] T. Sjostrand, S. Mrenna, and P. Z. Skands, *Comput. Phys. Commun.* **178**, 852 (2008).
- [52] J. de Favereau, C. Delaere, P. Demin, A. Giammanco, V. Lemaître, A. Mertens, and M. Selvaggi (DELPHES 3 Collaboration), *J. High Energy Phys.* **02** (2014) 057.
- [53] C. Han, K. i. Hikasa, L. Wu, J. M. Yang, and Y. Zhang, *J. High Energy Phys.* **10** (2013) 216.
- [54] C. Han, J. Ren, L. Wu, J. M. Yang, and M. Zhang, *Eur. Phys. J. C* **77**, 93 (2017).
- [55] M. R. Douglas, [arXiv:hep-th/0405279](https://arxiv.org/abs/hep-th/0405279); H. Baer, V. Barger, H. Serce, and K. Sinha, *J. High Energy Phys.* **03** (2018) 002.
- [56] H. Baer, V. Barger, J. S. Gainer, P. Huang, M. Savoy, D. Sengupta, and X. Tata, *Eur. Phys. J. C* **77**, 499 (2017).
- [57] See e.g., Report No. ATLAS Phys. PUB 2013-011; Report No. CMS Note-13-002.
- [58] H. Baer, A. Lessa, S. Rajagopalan, and W. Sreethawong, *J. Cosmol. Astropart. Phys.* **06** (2011) 031; K. J. Bae, H. Baer, and E. J. Chun, *Phys. Rev. D* **89**, 031701 (2014); H. Baer, V. Barger, and H. Serce, *Phys. Rev. D* **94**, 115019 (2016); K. J. Bae, H. Baer, and H. Serce, *J. Cosmol. Astropart. Phys.* **06** (2017) 024; H. Baer, V. Barger, D. Sengupta, and X. Tata, [arXiv:1803.11210](https://arxiv.org/abs/1803.11210).
- [59] T. Han, S. Mukhopadyay, and X. Wang, *Phys. Rev. D* **98**, 035026 (2018).
- [60] Talk by L. Shchutska, in *Review: The way forward for SUSY at LHC and beyond, Rencontres de Moriond, 2017, La Thuile, Italy* (unpublished), [https://indico.in2p3.fr/event/13763/contributions/15246/attachments/12662/15547/5\\_LesyaShchutska.pdf](https://indico.in2p3.fr/event/13763/contributions/15246/attachments/12662/15547/5_LesyaShchutska.pdf). See also Ref. [43].